Semicond. Sci. Technol. **23** (2008) 015001 (8pp) doi:10.1088/0268-1242/23/1/015001

Electronically-coupled up-conversion: an alternative approach to impurity photovoltaics in crystalline silicon

D Macdonald[1], K McLean[1], P N K Deenapanray[1], S De Wolf[2,4] and J Schmidt[3]

[1] Department of Engineering, College of Engineering and Computer Science, The Australian National University, Canberra, 0200 ACT, Australia
[2] Interuniversity Micro-Electronics Center (IMEC) vzw, Kapeldreef 75, B-3001 Leuven, Belgium
[3] Institut für Solarenergieforschung Hameln/Emmerthal (ISFH), Am Ohrberg 1, D-31860 Emmerthal, Germany

Received 6 June 2007, in final form 14 August 2007
Published 6 December 2007
Online at stacks.iop.org/SST/23/015001

Abstract
The traditional approach to harnessing the impurity-photovoltaic effect to improve solar cell performance is plagued by additional recombination caused by the impurity centres. This extra recombination channel is usually deemed to outweigh the benefits of additional generation of electron–hole pairs via sub-band-gap absorption through the impurity levels. Here we consider an alternative approach that restricts the impurity levels to a film with a wider band gap at the rear of a solar cell, isolating the impurities from the minority carriers generated in the base, but, in principle, still allowing impurity-generated carriers to contribute to the cell current. Initial proof-of-concept experiments show that implantation of silicon ions into amorphous silicon films on the rear of crystalline silicon wafers results in the desired increase in sub-band-gap absorptance of infrared photons, without degrading the surface passivation properties of the amorphous layer. However, these defect states are not thermally stable, and in any case do not result in additional carriers being injected into the silicon wafer itself, either because the infrared-generated carriers relax back to the valence band before the second photon can be absorbed, or because the free carriers recombine before reaching the wafer interface. Subsequent attempts involving implantation of iron and erbium impurities to generate stable absorption centres in the amorphous silicon films also failed to inject additional carriers into the crystalline wafer. Possible modifications that may alleviate these problems are discussed.

1. Introduction

In principle, the impurity-photovoltaic (IPV) effect provides a mechanism for generating additional electron–hole pairs via the absorption of two (or more) sub-band-gap photons via electronic states located within the band gap of the base of a solar cell. These photons would not normally be absorbed, meaning that the IPV effect can potentially lead to conversion efficiencies larger than the limiting efficiency for single-junction solar cells (approximately 29% for one-sun crystalline silicon solar cells [1]). This concept was originally introduced in 1960 by Wolf [2], and has been the subject of sporadic research over the intervening decades [3–12].

In practice, however, the intrinsic disadvantages of the IPV effect are quite often found to outweigh the benefits. The most important of these disadvantages is the fact that introducing states in the band gap also introduces a new recombination path. The loss of photo-generated carriers through this recombination channel may be greater than the gain in photo-generation through increased absorption. The impurities can also cause parasitic absorption of high-energy photons that would otherwise generate electron–hole pairs in their own right. An example is the use of indium impurities in silicon solar cells. Initial modelling suggested that these impurities may result in a modest efficiency improvement

[4] Present address: National Institute of Advanced Industrial Science and Technology (AIST), Central 2, 1-1-1 Umezono, Tsukuba, Ibaraki 305-8568, Japan.

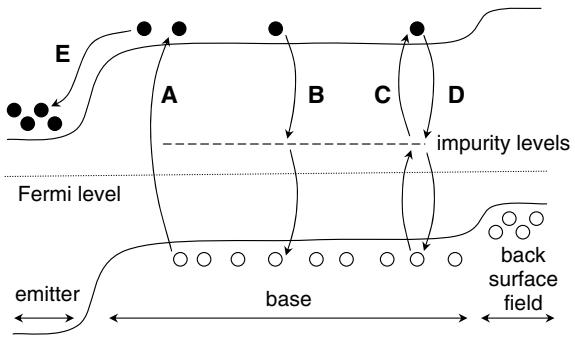

Figure 1. Schematic band diagram of a 'conventional' IPV cell (p-type base). A: normal photo-generation. B and D: impurity-mediated recombination. C: impurity-mediated generation. E: collection of minority carriers at the *p-n* junction.

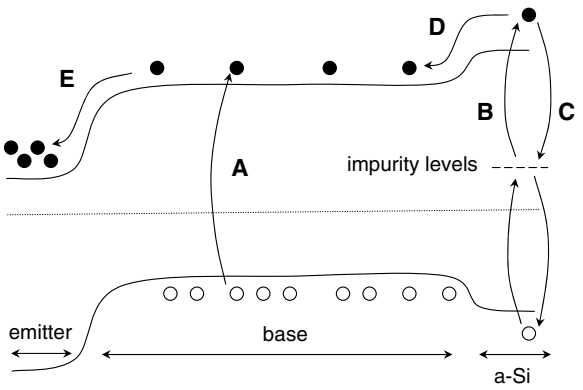

Figure 2. Schematic band diagram of the proposed alternative scheme (p-type base). A: normal photo-generation. B: impurity-mediated generation. C: impurity-mediated recombination. D: impurity-generated carriers entering the base. E: collection of minority carriers at the p–n junction.

[5, 6]. However, experimental attempts at boosting cell efficiency through the addition of indium evidently failed, although an improvement in infrared absorptance was clearly observed [6]. Subsequent modelling indicated that the negative impact of recombination through the indium levels outweighed the small increase in generation rate [8, 9]. More recent modelling has shown that similar conclusions are likely to hold for other localized impurity states in crystalline silicon as well [13].

It has been proposed that the use of impurity bands [14], rather than discrete states, may lead to reduced recombination losses, and therefore provide an overall performance gain. Also, it has been pointed out that the IPV effect deployed in larger band-gap materials has a better chance of succeeding than in materials such as crystalline silicon [11]. Nevertheless, the practical implementation of impurity bands and the development of new wide-gap materials for photovoltaics are major challenges. In this work, we elaborate on a recently introduced alternative approach to implementing impurity photovoltaics which in principle eliminates the recombination channel associated with the impurities, and also minimizes parasitic absorption losses [15]. This is achieved by isolating the impurities in a higher band-gap film at the rear of the cell, effectively screening them from minority carriers generated in the base. For reasons explained below, we refer to this concept as 'electronically-coupled up-conversion'. This paper also presents some initial experimental attempts to realize such an approach using a crystalline silicon base with an amorphous silicon (a-Si) film at the rear. We have attempted to achieve sub-band-gap absorption in the amorphous film by generating additional defects via self-implantation of silicon, or by adding impurities through implantation of Fe and Er.

2. Conceptual outline of electronically-coupled up-conversion

The conventional scheme for implementing the IPV effect is shown in the schematic band diagram of figure 1. Here we have shown a p-type solar cell with an n-type emitter at the front surface and a p^+ back-surface field. The deliberately-introduced impurity states are shown distributed throughout the base of the solar cell. The arrow labelled 'A' represents the generation of an electron–hole pair via absorption of a single photon with energy greater than the band gap, i.e. the normal generation process in a solar cell. The photo-generated minority carriers, which are electrons in the conduction band in this case, are then able to diffuse throughout the cell. They may be collected at the p–n junction, where they are swept down the potential slope (arrow 'E') and contribute to the cell current. Alternatively, they may recombine with holes before reaching the junction. For indirect band-gap semiconductors such as crystalline silicon, such recombination occurs largely through defect-related states, indicated in figure 1 as arrow 'B'. Introducing localized states for the IPV effect increases the concentration of such recombination centres, thus increasing the likelihood of minority carriers recombining before reaching the junction. On the other hand, these states can absorb a pair of infrared photons with energy well below the band gap, depicted as arrow 'C'. This additional generation is the basis for the IPV effect. Some of these generation events may be immediately reversed through recombination before the free electron can diffuse away from the impurity site, as shown in arrow 'D'. Clearly, whether the net effect of the IPV states is positive or negative for cell performance depends on the balance between extra generation and extra recombination. An additional negative effect not shown in figure 1 is the possibility of an impurity state absorbing a high-energy photon which could have otherwise generated an electron–hole pair via process 'A', a loss mechanism that may be referred to as parasitic absorption.

Figure 2 shows our alternative scheme for implementing the IPV effect. Here, the back-surface field has been replaced by a higher-band-gap material, which could be deposited as a thin-film. This is analogous to the rear side of Sanyo's HIT^{TM} cell, which features an a-Si/c-Si heterostructure on both surfaces [16]. In the experimental work that is presented in this paper, we have also used amorphous silicon for the rear film, with a band gap of around 1.6 eV. The impurity states are then restricted to this thin layer at the rear. Due to the higher band gap of the rear film and the resulting band

offset between the base and the rear film, carriers generated in the base cannot reach the impurity states to recombine. In other words, the impurity states are *electronically isolated* from minority carriers in the base. Of course, for any additional contribution to the overall cell current, it must be possible for minority carriers generated *within the film* at the rear, via the impurity states (arrow 'B'), to reach the base. This is indeed possible in the scheme depicted in figure 2, since such carriers can diffuse to the interface of the base and then be swept into the base courtesy of the band offset (arrow 'D'). Essentially then, this approach protects minority carriers generated in the normal fashion in the base from recombination through the impurity states, while still allowing impurity-generated carriers to potentially contribute to the cell current, providing they can reach the rear interface before recombining. This approach has another important advantage as well: there will be minimal parasitic absorption of visible and ultraviolet light in the a-Si layer because these photons will be almost completely absorbed at the front and in the base of the cell, before reaching the impurities. Note that our approach is different to the rear side of a HIT^{TM} cell, in the sense that, in the latter, the a-Si film at the rear acts only as a passivating film, and is therefore not an 'active' part of the device. On the other hand, the device that we propose contains additional impurity states in this rear film, with the intention of generating additional carriers.

There are some important requirements that the rear film of such a device must satisfy. It is essential that the film containing the impurity states also acts as an effective passivating film for the rear wafer surface, in order to avoid significant rear surface recombination. This is of course a requirement of any high-efficiency solar cell structure. This is one of the reasons for our choice of a-Si as the rear film material: it is known to provide very good surface passivation on crystalline silicon [17], as evidenced by the excellent performance of Sanyo's HIT^{TM} cells [16]. Another constraint on the rear film is that its band gap should be sufficiently large to allow a band offset at the conduction band that is large enough to exclude minority carriers from the base, while also maintaining a valence band offset (or at least flat-band conditions) for majority carriers. This is important for maintaining charge neutrality in the amorphous film. This implies that the rear film should be p-type or intrinsic for the case of a p-type base as shown in figure 2. On the other hand, the band gap should not be too much larger than the base, since then the number of infrared photons of sufficient energy to cause two-step generation is reduced. For example, it is easy to imagine that if the band gap of the rear film is more than twice the band gap of the base, then there will be very few photons available that could promote a two-step generation event through a mid-gap state, since such photons would have already been absorbed in the base itself. (In this case a three-step generation event is in principle possible, but is much more prone to relaxation to lower states before the carriers are fully promoted to the conduction band). Amorphous silicon was chosen for the experiments in this work as it has a band gap that seems to be a reasonable compromise between these competing requirements.

Of course, the diffusion length of minority carriers in a-Si films is short, and the presence of the impurity states will reduce it even further. Consequently, the probability of any carriers generated in the a-Si layer reaching the base may be very low. However, even if only a small proportion reaches the base, the extra carriers will cause an increased current, *without* the risk of reducing the electronic performance of the base. The optical properties of the rest of the cell should also be almost unperturbed, since parasitic absorption of ultraviolet and visible light will be very low. There will, however, be some parasitic loss of near-infrared photons that could otherwise be absorbed in the base after multiple passes through the cell (in other words, it may reduce the gains from light-trapping). In comparison to a standard cell, the proposed scheme therefore should cause no electronic losses (recombination), and only minor optical losses (parasitic near-infrared absorption). These would hopefully be offset by the increase in current due to the IPV-generated carriers injected from the a-Si layer.

This approach may be thought of in terms of up-conversion [18]. The a-Si layer in fact operates as an up-converter of infrared light passing through the cell. However, in contrast to conventional up-converters, which re-emit high-energy photons back into the cell, in this case the photo-generated carriers diffuse directly into the base. In this sense, the proposed scheme might be referred to as an 'electronically-coupled' up-converter, rather than the traditional 'optically-coupled' up-converter. In principle, avoiding the need to re-emit a high-energy photon may be an advantage, since this process is often rather inefficient in optically-coupled up-converters. On the other hand, the diffusion of impurity-generated carriers through a highly-defected amorphous film may also be inefficient.

2.1. Potential gains

It is relatively straightforward to perform a rough estimate of the potential gains in cell current that may be achievable through this concept. Approximately 38% of photons in the AM1.5 spectrum [19] have energy below the band gap, 1.12 eV, of crystalline silicon. If we consider a mid-gap state at 0.8 eV for the two-step process in the a-Si layer (with band gap of 1.6 eV), only photons with energy greater than this, and below the crystalline silicon band gap, may be absorbed through the IPV effect described here. This represents approximately 16% of the total photon flux. If all such photons were absorbed without recombination in the a-Si layer, this would correspond to a boost in short-circuit current of approximately 5 mA cm^{-2} for a two-step process.

This is a simplistic calculation that ignores free-carrier absorption and distributed defect energy levels, but it is sufficient to give an idea of the maximum potential gains. However, it must be conceded that there are a number of loss mechanisms that will significantly reduce the current gain to below 5 mA cm^{-2}. Firstly, there will be incomplete absorption of infrared photons, which will be governed largely by the optical cross sections of the impurity states and their spatial distribution in the rear film. Secondly, some absorption

processes that promote a carrier to the mid-gap states will be followed by relaxation back to the valence band before a second photon is absorbed to inject the carrier into the conduction band. Finally, even those carriers that *do* make it to the conduction band will be prone to recombination via either the introduced impurity states or other defects native to the amorphous material. All of these loss mechanisms are likely to be significant. However, even if up to 80% of the potential current gain is lost, the resulting current increase may still justify the use of such an approach, if it were not overly complex to implement.

Recently, more sophisticated modellings of the potential gains of the electronically-coupled up-converter have been published [20, 21]. These have confirmed that the potential gains are rather modest, but nonetheless superior to the conventional IPV approach in many cases. In the ideal case of no recombination through the defect states, the efficiency limit for a non-concentrating single-junction crystalline silicon solar cell was found to increase from around 30% to 36% when an electronically-coupled up-converter (an a-Si film containing impurities offset by 0.5 eV from the band edge) was included. In comparison, a similar conventional IPV approach yielded a maximum efficiency of around 31%. In the more realistic case, where reasonable rates of recombination through the defect states are included via the Shockley–Read–Hall model, the advantage over the single-junction limit was reduced, but nevertheless remained significantly higher than the corresponding limit for conventional IPV cells for base band-gaps of below 2.5 eV. The modelling confirmed that, in general, the electronically-coupled up-converter was less sensitive to impurity-mediated recombination than the conventional IPV approach, especially for smaller band-gap base materials such as crystalline silicon. The reader is referred to [20, 21] for more details on estimating the potential gains of the approach described here. The purpose of this paper is to report our initial attempts to realize such a device experimentally.

2.2. Practical aspects

There are several practical factors which need to be considered when hoping to maximize the desired IPV effect. In this work, defect states are introduced in the a-Si film by ion-implantation. This may result in an increase in infrared absorption via two mechanisms: through an increased dangling bond/defect density caused by ion-induced damage, or by the chemical presence of the added ions themselves. However, these sub-band-gap absorption processes in the a-Si layer are likely to be quite weak, requiring multiple passes through the layer. This means good light-trapping (front surface texturing) is necessary.

Secondly, the a-Si layer should be kept thin enough to allow efficient extraction of carriers into the base, especially considering that the presence of introduced defects/impurities will reduce the diffusion length there. On the other hand, it must be thick enough to allow implantation without damaging the a-Si/c-Si interface or contaminating the base. Low-energy implants can be performed to produce a profile with peak concentrations less than 50 nm deep, but considering the straggle of these profiles, we initially chose a 'safe' thickness of 150 nm for the a-Si layer. Subsequent experiments were performed with thinner 70 nm films.

Finally, any IPV-generated carriers from the a-Si layer which do enter the base will need to diffuse to the front of the device for collection by the emitter. This implies that the diffusion length in the base must be significantly longer than the base thickness.

Assuming that the as-deposited wafers have sufficient surface passivation and bulk diffusion lengths, there are three experimental checks which must be satisfied in order for the desired IPV effect to occur. Firstly, there must be a measurable *increase in the sub-band-gap absorptance* after implantation (here absorptance is defined as the ratio of the number of photons absorbed to the number of photons incident on the sample at a given wavelength). This would indicate that the impurity or defect states are absorbing sub-band-gap photons, but not necessarily that this results in extra carriers in the conduction band, or that these are able to diffuse to the base. Secondly, the implantation *must not adversely affect the surface passivation* at the rear a-Si/c-Si interface. Finally, there should be an *increase in the infrared photoconductance* of the wafer under sub-band-gap illumination. This would indicate that IPV-generated carriers are promoted to the conduction band of the amorphous film, and then indeed diffuse to the base, where they add to the infrared conductance. If these three conditions can be satisfied, then there appears to be a good chance of realizing improved cell performance with such an approach. As described below, the attempts presented in this paper have satisfied the first two tests. The last step has however proved difficult to achieve.

3. Experimental details

Boron-doped float-zone (FZ) wafers were chosen for these experiments due to their long bulk diffusion length. To provide good infrared light-trapping, the wafers were initially alkaline textured on both surfaces. For the experiments with Si and Fe implants, 0.8 Ω cm wafers of 280 μm thickness were then oxidized at 1100 °C followed by a forming gas anneal at 400 °C. The oxide layer serves the dual purposes of reducing front surface reflection and providing good front surface passivation. The oxide layer and texturing were removed from the rear surface, and 150 nm thick, nominally intrinsic a-Si films were deposited on the rear surface by plasma-enhanced chemical vapour deposition (PECVD) at IMEC. These depositions were performed with a parallel-plate direct Oxford Plasmalab reactor operated at 13.56 MHz and with a 230 mm diameter electrode. The substrate temperature during deposition was estimated to be 190 °C, the process pressure was 0.525 Torr, the silane gas flow rate was 100 sccm and the microwave power was initially 10 W for 2 s and then 6 W for the remainder of the deposition. The deposition rate was approximately 0.9 Å s^{-1}. Ion-implantation into the a-Si layer of either Si^{28} or Fe^{56} ions was performed through a 3 cm square aperture. Ion energies between 15 keV and 60 keV were used for Si, giving peak implantation depths between

24 and 87 nm, as modelled using TRIM [22]. Si-ion doses varied between 10^{12} and 10^{16} cm^{-2}. For the Fe implants, an energy of 40 keV was used (36 nm depth), with doses ranging between 10^{12} and 10^{14} cm^{-2}. Low ion currents for Fe prohibited the use of higher doses.

A further set of samples were prepared for Er^{166} implantation. In this case, the textured FZ wafers (200 Ω cm) were deposited on both sides with nominally intrinsic, 70 nm thick a-Si using a PECVD reactor at ISFH. These films were made thinner than in the previous experiment in the hope of allowing more IPV-generated carriers to reach the base, as discussed below. The depositions were performed with the same model of Oxford Plasmalab PECVD reactor as described above. In this case, the substrate temperature during deposition was set at 225 °C, the process pressure was 0.45 Torr, the silane gas flow rate was 30 sccm and the microwave power was 100 W. The deposition rate was approximately 5 Å s^{-1}. Er was implanted into the a-Si films in the form of ErO^- ions with beam energies between 50 and 90 keV, and a dose of 10^{13} cm^{-2} (again a low ion yield limited the achievable dose). The ion source was a 1:1 mixture of Er_2O_3 and Mo powders to prevent charging. The Er and O ions should split upon entering the Si matrix [23], meaning that the resulting energies of the Er ions are about 10% less than the total beam energy. This corresponds to Er peak-implant depths between 28 and 42 nm. The peak depth of the O ions is somewhat less in each case, meaning that it should not damage the interface if the Er does not.

The absorptance (the proportion of photons absorbed in the sample) was measured via transmittance (proportion of photons transmitted) and reflectance (proportion of photons reflected) measurements, using a Carey spectrophotometer with an integrating sphere, over the wavelength range of 300–1800 nm. The reflectance (R) was measured by placing the sample directly behind the integrating sphere so that all light reflected from the sample (including any light that penetrated into the sample and re-emerged from the front surface, for example after reflection from the rear surface), was randomized and detected. The transmittance (T) was measured by placing the sample directly in front of the integrating sphere, allowing any light transmitted through the sample to be randomized and detected. The absorptance (A) at a given wavelength was then calculated via $A = 1 - T - R$. By measuring the absorptance in this way in a sample before and after implantation into the a-Si film on the rear, any change in absorptance can be attributed to absorption through implant-related defects.

Lifetime and photoconductance measurements were performed using the quasi-steady-state photoconductance (QSSPC) method [24]. The a-Si films were found to provide good rear surface passivation in the as-deposited state. For the first set of a-Si depositions on 0.8 Ω cm wafers, the effective lifetime measured at an excess carrier concentration of 10^{15} cm^{-3} was 100 μs, corresponding to a minority carrier bulk diffusion length of around 500 μm, significantly longer than the wafer thickness, as required. The second set of depositions yielded effective lifetimes above 1 ms (due to the higher resistivity), also easily satisfying the surface passivation and diffusion length requirements. Infrared photoconductance measurements were performed using a thick (800 μm) intrinsic silicon wafer as an optical filter.

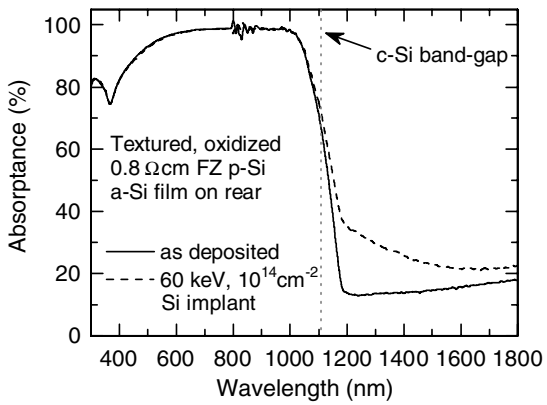

Figure 3. Absorptance as a function of wavelength for a sample before and after 60 keV, 10^{14} cm^{-2} Si implantation. The band gap of crystalline silicon is shown. Additional sub-band-gap absorptance at higher wavelengths is evident after implantation.

4. Results and discussion

4.1. Absorptance measurements

Figure 3 shows absorptance data for one of the 0.8 Ω cm samples before and after a 60 keV Si implant with a dose of 10^{14} cm^{-2}. In the as-deposited sample, a small amount of free-carrier absorption, due to the doping, is observable above the crystalline silicon band gap, which increases in strength approximately quadratically with wavelength. However, the Si-implanted sample displays additional infrared absorptance. This is most likely related to the presence of band-gap states in the a-Si layer, and is precisely the type of absorptance increase that we wish to observe. Indeed, it is well known that implantation of a-Si leads to additional defect states [25], as has been shown, for example, by optical absorption measurements similar to our own [26], electron paramagnetic resonance studies [27] and conductivity measurements [28]. Figure 4 shows the change in absorptance due to the defect states, for the 24 keV Si implants, which peaks at around 1185 nm, and increases with the Si-ion dose before saturating at doses above 10^{15} cm^{-2}.

Figure 5 plots the additional absorptance at 1185 nm as a function of dose for both Si and Fe implants of the same depth (and hence similar damage). The results clearly show that the amount of extra absorptance is *independent* of the implanted species. This implies that the absorption centres introduced through the implantation damage dominate the measurements, rather than absorption through the added atoms themselves. This is corroborated by the absorptance data in figure 6, which show that the extra absorptance (shown on the left axis) actually increases with the implantation energy (or depth) for a fixed ion dose. Note that if it were only the added atoms that caused the additional absorptance, then the implant energy should not affect the amount of absorption. On the other hand, if the damage causes the absorption, then implantation with

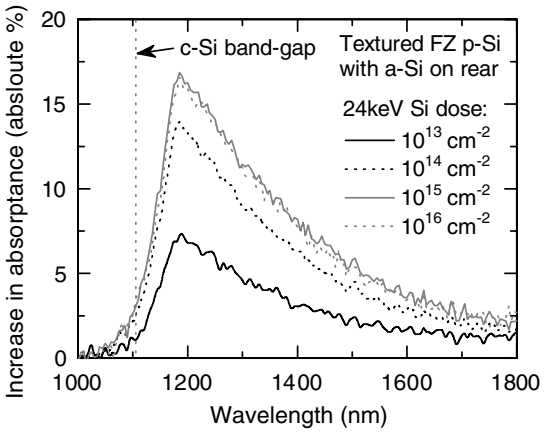

Figure 4. Increase in absorptance as a function of wavelength for various doses of 24 keV Si implants.

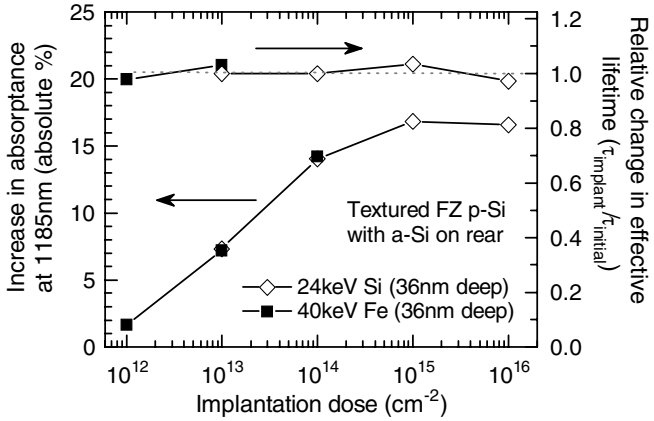

Figure 5. Increase in absorptance at 1185 nm and change in effective lifetime as a function of ion dose for 36 nm deep Si (24 keV) and Fe implants (40 keV).

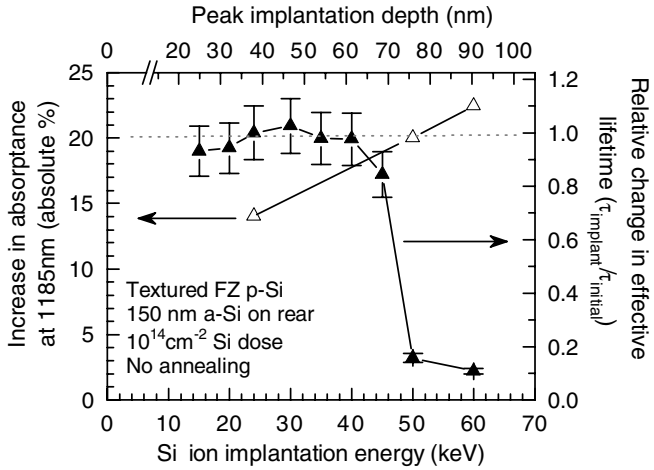

Figure 6. Increase in absorptance at 1185 nm (left axis) and relative change in effective lifetime (right axis) as a function of ion energy (bottom axis) or peak implant depth (top axis) for Si implants with a dose of 10^{14} cm^{-2}.

higher energy should lead to greater absorption, as it will cause greater damage.

This conclusion is also supported by the thermal instability of the absorption centres. Annealing at various

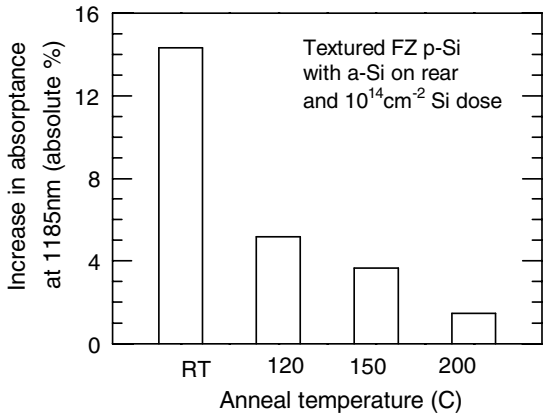

Figure 7. Reduction in the additional absorptance at 1185 nm after annealing for 60 min at various temperatures for the 24 keV Si implant with a dose of 10^{14} cm^{-2}.

low temperatures (up to 200 °C) for 60 min, as shown in figure 7, deactivates the implant-related absorption centres, as has been observed previously [26]. This is also similar to the well-known annealing behaviour of the degradation in a-Si p–i–n cells, referred to as the Staebler–Wronski effect, and attributed to the action of dangling bonds. Light-activated degradation of such cells is reversed upon annealing at moderate temperatures. The similar annealing behaviour suggests that the absorption centres observed here may be due to dangling bonds also, which are caused by the implantation damage. In addition to low temperature annealing, leaving a sample at room temperature for several months after implantation also caused a gradual reduction in the additional absorptance.

4.2. Surface passivation measurements

For efficient devices, the surface passivation at the rear interface should remain unchanged by implantation. Figure 5 (right axis) shows the ratio of the carrier lifetime measured before and after implantation for the relatively shallow (36 nm peak implant depth) Si and Fe implantations, as a function of dose. Clearly, the lifetime remains unchanged, even for the highest doses, indicating that the interface surface passivation properties are not affected by the implantation, as required. This is as expected for these shallow implants in a 150 nm thick film.

For deeper implants, we expect there will be an energy for which a large enough fraction of the implanted ions reach the interface and degrade the surface passivation. Figure 6, the right hand axis, shows that this does indeed occur abruptly for energies of 45 keV and above for Si ions. This energy corresponds to an implant depth of 66 nm with a straggle of 27 nm. The interface is approximately three 'straggles' away from the peak implantation dose in this case, which should serve as a rule of thumb for other species also, if the same or lower ion doses are used.

4.3. Infrared photoconductance measurements

The final test is whether the absorbed infrared photons result in extra free carriers in the a-Si layer, and whether

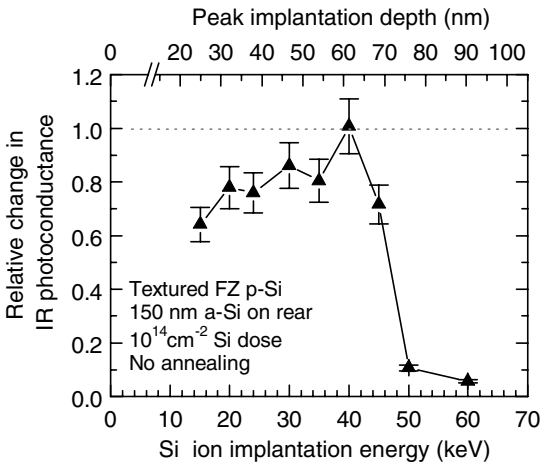

Figure 8. Relative change in infrared photoconductance as a function of ion energy (bottom axis) or peak implant depth (top axis) for Si implants with a dose of 10^{14} cm^{-2}.

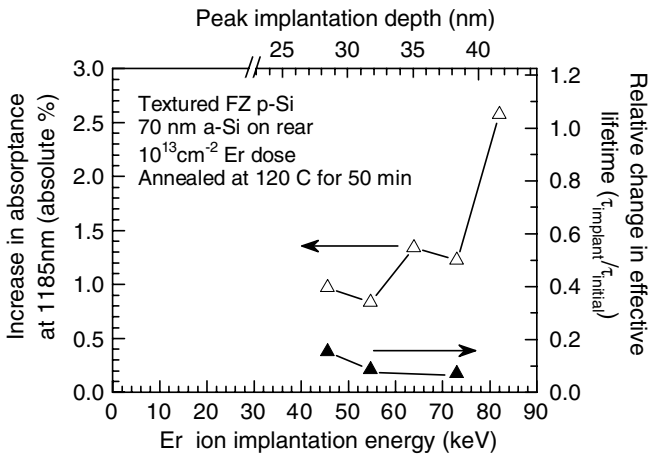

Figure 9. Increase in absorptance at 1185 nm (left axis) and relative change in effective lifetime (right axis) as a function of ion energy (bottom axis) or peak implant depth (top axis) for Er implants with a dose of 10^{13} cm^{-2}.

these subsequently reach the base before recombining. By measuring the photoconductance of the wafer under infrared light, we can check if there are extra carriers in the base of the implanted samples compared to non-implanted controls. This is much more sensitive than measuring under white light, since the carriers generated in the base itself then swamp the measurements.

The results are shown in figure 8 for Si implants. For the shallower implants, the IR photoconductance decreases after implantation. This is most likely due to parasitic absorption of near-IR light which would otherwise be weakly absorbed in the base. However, for deeper implants, the conductance seems to recover towards the control value, although the data are somewhat noisy. This suggests that the closer proximity of the defects to the rear interface allows more carriers generated in the a-Si to reach the base, compensating the loss due to parasitic absorption. This effect is small though, and the IR conductance never actually exceeds that of the control, as required for a boost to the cell current. Nevertheless, it may provide some indirect evidence of a small number of carriers generated by the two-step absorption process reaching the base.

Clearly, the relatively large increase in infrared absorptance we observe does not translate to extra minority carriers reaching the base. This may be due to incomplete two-step absorption—i.e. carriers relaxing back to the valence band of the amorphous layer from the defect state before another photon is absorbed to promote the carrier to the conduction band. This would indicate a poor combination of optical and electronic cross sections for the defect states used in this work. Alternatively, if minority carriers are indeed generated in the amorphous film via the two-step process, they may recombine at impurity centres or other defects in the film before reaching the interface with the base.

The unstable nature of the infrared absorption centres generated by the Si implants was the motivation for performing the Fe implants. The apparent failure of the Fe atoms to generate absorption centres in their own right, at least for the concentrations achieved here, led us to also trial Er as a possible impurity candidate. The results for the Er implants are shown in figure 9, in analogy to figure 6 for the Si implants. The samples were annealed at 120 °C for 60 min prior to measurement, in order to remove most of the absorption-centres caused by the implant damage. This should make it possible to detect any Er-related absorption centres. However, as figure 9 shows, the measured increase in absorptance was very small, and the fact that it increases with implant energy implies that even these absorption centres are caused by residual damage, and are not due to the Er ions themselves. Figure 9 also shows that the effective lifetime was significantly degraded after implantation. These samples had thinner a-Si films (around 70 nm instead of 150 nm), in an attempt to generate carriers closer to the interface with the base. However, it seems that the implantation has resulted in significant damage to the interface, despite the fact that the peak implant depth was kept well below the film thickness. This may reflect non-uniformity in the a-Si film thickness in these samples. In any case, as for Fe, the Er implants did not result in additional absorptance in the infrared, and so would not lead to improved performance, even in the absence of damage to the rear passivation. It may be that higher concentrations of metals such as Fe and Er are required to cause significant absorption in the a-Si layers, but these are not easily achieved with implantation. This might be possible in future by incorporating the impurities into the layer during deposition.

There are several options for future work. Other impurities may have a better balance between optical absorption strength and recombination activity than the dangling bonds used. However, our attempts with implanted Fe and Er impurities have not been successful. Alternatively, it may be better to 'grow-in' the impurities, which may allow better control of the impurity profile, yielding a higher concentration of impurities closer to the interface. To help with free-carrier extraction from the amorphous film, it may be beneficial to include graded doping in the a-Si layer to achieve a drift field. Also, the infrared

photoconductivity measurements here were performed with an intensity similar to the infrared part of the one-sun solar spectrum. Under more intense light, such as in concentrating systems, the probability of completing the two-step absorption process before relaxation back to the valence band, may be significantly increased. Finally, better results may be achievable with materials other than the combination used here of amorphous and crystalline silicon. In fact, recent modelling has shown that the potential benefits of this approach are greater when a larger band-gap material is used for the base (around 2.0 eV seems close to optimal) [20].

5. Conclusions

We have described an alternative approach to implementing the IPV effect in crystalline silicon, referred to as electronically-coupled up-conversion. It avoids two of the major problems associated with the conventional IPV approach—namely, recombination of minority carriers generated in the base by a single photon, and parasitic absorption. Initial attempts using implantation-induced dangling bonds as the defect states in an amorphous silicon film have revealed significant increases in the infrared absorptance, while avoiding damage to the a-Si/c-Si interface. However, we have not observed significant increases in the photoconductance of the base, indicating that few, if any, of the impurity-generated carriers actually reach the base. This suggests that these absorption centres may be very strong recombination centres, or alternatively, the amorphous films are of poor bulk quality. Attempts to use implanted Fe and Er ions to generate less recombination-active absorption centres in the a-Si film did not result in additional absorptance. The maximum potential gains in terms of cell performance of this approach are relatively modest, less than 5 mA cm^{-2}. However, considering that a-Si films are already being used to passivate the rear surface of solar cells [29], some in commercial production [16], it has the potential to be relatively easy to implement in practice.

Acknowledgments

This work has been supported by the Australian Research Council. The authors are grateful to C Holly for help with sample preparation, J Mitchell for assistance with some measurements, and A Cuevas and P Altermatt for helpful discussions. Professor R Elliman kindly provided access to the ion implanter at the Research School of Physical Science and Engineering, ANU.

References

[1] Kerr M J, Cuevas A and Campbell P 2003 *Prog. Photovolt. Res. Appl.* **11** 97–104
[2] Wolf M 1960 *Proc. IRE* **48** 1246–63
[3] Güttler G and Queisser H J 1970 *Energy Convers.* **10** 51
[4] Würfel P 1993 *Sol. Energy Mater. Sol. Cells* **29** 403–13
[5] Keevers M J and Green M A 1994 *J. Appl. Phys.* **75** 4022–31
[6] Keevers M J and Green M A 1996 *Sol. Energy Mater. Sol. Cells* **41/42** 195–204
[7] Kasai H and Matsumura H 1997 *Sol. Energy Mater. Sol. Cells* **48** 93–100
[8] Schmeits M and Mani A A 1999 *J. Appl. Phys.* **85** 2207–12
[9] Karazhanov S Z 2001 *J. Appl. Phys.* **89** 4030–6
[10] Green M A 2001 *Prog. Photovolt. Res. Appl.* **9** 137–44
[11] Beaucarne G, Brown A S, Keevers M J, Corkish R and Green M A 2002 *Prog. Photovolt. Res. Appl.* **10** 345–53
[12] Brown A S and Green M A 2002 *J. Appl. Phys.* **92** 1329–36
[13] Harder N P and Würfel P 2004 *Proc. 19th Eur. Photovoltaic Solar Energy Conference (Paris)* (Munich: WIP) pp 84–7
[14] Luque A and Marti A 1997 *Phys. Rev. Lett.* **78** 5014–7
[15] Macdonald D, McLean K, Mitchell J, Deenapanray P N K and DeWolf S 2004 *Proc. 19th Eur. Photovoltaic Solar Energy Conference (Paris)* (Munich: WIP) pp 88–91
[16] Taguchi M, Kawamoto K, Tsuge S, Baba T, Sakata H, Morizane M, Uchihashi K, Nakamura N, Kiyama S and Oota O 2000 *Prog. Photovolt. Res. Appl.* **8** 503–13
[17] Dauwe S, Schmidt J and Hezel R 2002 *Proc. 29th IEEE Photovoltaic Specialists Conf. (New Orleans, LA)* (New York: IEEE) pp 1246–9
[18] Trupke T, Green M A and Würfel P 2002 *J. Appl. Phys.* **92** 4117–22
[19] Green M A 1998 *Solar Cells* (Kensington, NSW: The University of New South Wales)
[20] Harder N P and Macdonald D 2005 *Proc. 31st IEEE Photovoltaic Specialists Conf. (Orlando, FL)* (New York: IEEE) pp 110–3
[21] Harder N P 2005 *Proc. 20th Eur. Photovoltaic Solar Energy Conf. (Barcelona, Spain)* (Munich: WIP) pp 302–5
[22] Biersack J P and Ziegler J F 1995 Transport of Ions in Matter (TRIM), Version 95.06
[23] Sachdeva R, Istratov A A, Deenapanray P N K and Weber E R 2005 *Phys. Rev.* B **71** 195208
[24] Sinton R A and Cuevas A 1996 *Appl. Phys. Lett.* **69** 2510–2
[25] Roorda S, Sinke W C, Poate J M, Jacobson D C, Dierker S, Dennis B S, Eaglesham D J, Spaepen F and Fuoss P 1991 *Phys. Rev.* B **44** 3702–25
[26] Zammit U, Madhusoodanan K N, Marinelli M, Scudieri F, Mercuri F, Wendler E and Wesch W 1995 *Nucl. Instrum. Methods Phys. Res.* B **96** 241–4
[27] Pivac B, Rakvin B and Reitano R 1999 *Nucl. Instrum. Methods Phys. Res.* B **147** 132–5
[28] Coffa S, Priolo F and Battaglia A 1993 *Phys. Rev. Lett.* **70** 3756–9
[29] Dauwe S, Mittelstädt L, Metz A, Schmidt J and Hezel R 2003 *Proc. 3rd World Conf. on Photovoltaic Energy Conversion (Osaka, Japan)* (New York: IEEE) pp 1395–8